NIH Public Access
Author Manuscript
Acta Biomater. Author manuscript; available in PMC 2013 August 01.

Published in final edited form as:
Acta Biomater. 2012 August ; 8(8): 3138–3143. doi:10.1016/j.actbio.2012.04.022.

Micromechanical finite element modeling and experimental characterization of the compressive mechanical properties of polycaprolactone:hydroxyapatite composite scaffolds prepared by selective laser sintering for bone tissue engineering

Shaun Eshraghi and **Suman Das***
George W. Woodruff School of Mechanical Engineering 801 Ferst Drive Georgia Institute of Technology Atlanta, GA 30332-0405, U.S.A.

Abstract

Bioresorbable scaffolds with mechanical properties suitable for bone tissue engineering were fabricated from polycaprolactone (PCL) and hydroxyapatite (HA) by selective laser sintering (SLS) and modeled by finite element analysis (FEA). Both solid gage parts and scaffolds having 1-D, 2-D and 3-D orthogonal, periodic porous architectures were made with 0, 10, 20 and 30% HA by volume. PCL:HA scaffolds manufactured by SLS had nearly full density (99%) in the designed solid regions and had excellent geometric and dimensional control. Through optimization of the SLS process, the compressive moduli for our solid gage parts and scaffolds are the highest reported in the literature for additive manufacturing. The compressive moduli of solid gage parts were 299.3, 311.2, 415.5 and 498.3 MPa for PCL:HA loading at 100:0, 90:10, 80:20 and 70:30 respectively. The compressive effective stiffness tended to increase as the loading of HA was increased and the designed porosity was lowered. In the case of the most 3-D porous scaffold, the compressive modulus more than doubled from 14.9 MPa to 36.2 MPa when changing the material from 100:0 to 70:30 PCL:HA. A micromechanical finite element analysis (FEA) model was developed to investigate the reinforcement effect of HA loading on the compressive modulus of the bulk material. Using a first-principles based approach, the random distribution of HA particles in a solidified PCL matrix was modeled for any loading of HA to predict the bulk mechanical properties of the composites. The bulk mechanical properties were also used for FEA of the scaffold geometries. Results of the FEA were found to be in good agreement with experimental mechanical testing. The development of patient and site-specific composite tissue engineering constructs with tailored properties can be seen as a direct extension of this work on computational design, *a priori* modeling of mechanical properties and direct digital manufacturing.

Keywords

tissue engineering; scaffolds; polycaprolactone; hydroxyapatite; selective laser sintering; mechanical properties

© 2012 Acta Materialia Inc. Published by Elsevier Ltd. All rights reserved

*Corresponding author: sumandas@gatech.edu.

Publisher's Disclaimer: This is a PDF file of an unedited manuscript that has been accepted for publication. As a service to our customers we are providing this early version of the manuscript. The manuscript will undergo copyediting, typesetting, and review of the resulting proof before it is published in its final citable form. Please note that during the production process errors may be discovered which could affect the content, and all legal disclaimers that apply to the journal pertain.

NIH-PA Author Manuscript
NIH-PA Author Manuscript
NIH-PA Author Manuscript

NIH-PA Author Manuscript

NIH-PA Author Manuscript

NIH-PA Author Manuscript

1. INTRODUCTION

Additive manufacturing is a promising emerging field of research for the manufacture of bioresorbable scaffolds in tissue engineering of skeletal defects. Bioresorbable scaffolds are used in bone tissue engineering to act as a controlled extracellular environment where the cells can attach, differentiate and regenerate tissue. Additive manufacturing methods enable control over the microarchitecture of the scaffold which in turn dictates the geometry of the newly formed tissue.

Selective Laser Sintering (SLS) is a laser-based additive manufacturing technique in which an object is built layer-by-layer using powdered materials, radiant heaters and a computer controlled laser [1]. In SLS, the digital representation of an object is mathematically sliced into a number of thin layers. The object is then created by scanning a laser beam and selectively fusing (melting or sintering) patterns into sequentially deposited layers of a powder. Each patterned layer of powder is also fused to its underlying layer and corresponds to a cross-section of the object as determined from the mathematical slicing operation. This layered manufacturing method allows the fabrication of scaffolds with a high degree of geometric complexity and enables the direct conversion of a scaffold's computer model into its physical realization—allowing patient-specific and tissue-specific reconstruction strategies to be easily developed [2–10].

In previous work [11], we demonstrated the ability of SLS to produce viable polycaprolactone (PCL) scaffolds for bone tissue engineering; however, the scaffolds had some manufacturing induced porosity (20%) and only moderate geometric control. We later improved the processing parameters for the SLS of PCL and were able to produce scaffolds with nearly full density (>95%) and better geometric control (3–8%) [12]. Recently, we showed that parts manufactured by SLS with optimized processing parameters could have properties matching those made by conventional techniques such as injection or compression molding and that computationally designed scaffolds had mechanical properties that were predictable through finite element analysis (FEA) [13].

Calcium phosphates (CaP), such as tricalcium phosphate (TCP) and hydroxyapatite (HA), are bioactive molecules that are inorganic components of bone matrix. They are involved in protein adsorption, bone cell attachment and apatite deposition [14]. There have been conflicting reports in the literature about the beneficial effect of HA in composite scaffolds. Some reports in the literature claim that HA has a beneficial affect [15–17] while other reports did not show any significant change with the loading of HA in composites [18, 19]. Because of their brittleness, CaPs have poor mechanical properties in torsion and bending; however, there are many reports in the literature showing that loading ceramics up to 30% in polymer composites can improve their mechanical properties [20–22].

SLS of composite materials has been discussed in the literature but there is limited published data on the compressive mechanical properties of SLS-processed PCL composites with near-full density in designed solid regions. Composites of PCL and HA have been investigated recently by two groups. Wiria et al. [23] fabricated solid PCL:HA specimens with 10, 20 and 30 wt.% HA and obtained compressive Young's moduli of 33.91, 23.59 and 56.62 MPa respectively. Eosoly et al. [20] fabricated scaffolds with 67% porosity and obtained a compressive Young's modulus of 2.3 MPa and yield strength of 0.6 MPa in PCL:HA with 30% HA loading by weight.

Other additive manufacturing methods such as precision extrusion deposition (PED) and fused deposition molding (FDM) have been used to manufacture neat PCL and PCL composite scaffolds. Domingos et al. [24] reported a compressive modulus of 79.1 MPa for 49% porous PCL scaffolds fabricated by extrusion. Shor et al. [25] reported Young's moduli

NIH-PA Author Manuscript

NIH-PA Author Manuscript

NIH-PA Author Manuscript

of 84 and 76 MPa for 60 and 70% porous scaffolds, respectively, fabricated by PED with 25% wt. HA. Lam et al. [26] reported a Young's modulus of 6.77 MPa and yield stress of 0.99 MPa for PCL scaffolds loaded with 20% wt. HA fabricated by FDM. Conventional manufacturing techniques have also been employed; Azevedo et al. [22] reported Young's moduli of 350 to 600 MPa for PCL:HA composites at 0 to 30% wt. after compression molding.

Here we report on the manufacture of fully dense PCL:HA composite scaffolds with up to 30% filler loading by volume. Because ceramic fillers act to impede the process of particle coalescence and densification, manufacturing parts that are fully dense is difficult and to our knowledge, we are the only group to report on fully dense PCL:HA scaffolds. We also develop a first principles micromechanical model to predict the properties of composites using known filler loading. Using the output of the micromechanical model it is possible to predict the mechanical properties of the scaffolds at any filler loading. We verify the accuracy of our model with mechanical property testing. The ability of SLS to manufacture anatomic shaped scaffolds with designed microarchitecture out of bioactive and bioresorbable composite materials at high filler loading can be considered an extension of this work [11–13].

2. MATERIALS AND METHODS

The hydroxyapatite (HA), used as filler, was provided by Astaris (St. Louis, MO). HA is a calcium apatite with molecular formula $Ca_{10}(OH)_2(PO_4)_6$ and molecular weight Mn=1004. The appearance of HA is a white powder with average particle size of 45μm. The crystallinity characteristics of HA (Figure 1) were assessed by X-ray diffraction (XRD) in a X'Pert powder diffractometer (PANanalytical B.V., Almelo, The Netherlands) using monochromatic, filtered Cu-Kα (λ=1.5405 Å) radiation. Polycaprolactone (PCL) marketed by Solvay Caprolactones (Warrington, UK) under the brand name CAPA® 6501 (Solvay Caprolactones has since been acquired by Perstorp, Sweden) was used as the polymer matrix. PCL is a semicrystalline (56%) aliphatic thermoplastic having a melting point of 58–60°C and a glass transition temperature of approximately −60°C [27]. Gel Permeation Chromatography (GPC) analysis (THF, 25°C) was conducted to determine the molecular weight of CAPA® 6501 both before and after processing (pre-processed PCL: M_n = 91,900 ± 7,700; post-processed PCL: M_n = 73,000 ± 6,300). Mechanical test sieving conducted according to ISO 2591-1 standards confirmed that the powder has an average particle size of 90μm and a distribution in which 98% of all particles are less than 125μm in size (no particles > 150μm).

PCL:HA powders were mixed in a dry state using a rotary tumbler (784 AVM, U.S. Stoneware, Ohio) for 24 hours. This mixing protocol has been shown to provide dispersion for other composite material systems [28–31]. The PCL:HA powder was processed using a Sinterstation® 2000 commercial SLS machine (3D Systems Inc., Valencia, CA). Preheated and sequentially deposited powder layers were scanned using a low power continuous wave CO_2 laser (λ=10.6μm, power <10W) focused to a 450μm spot. Further details on SLS processing and process parameter selection are reported elsewhere [12].

Scaffold Design and Fabrication

Scaffolds with 1D, 2D and 3D orthogonal porous square channels measuring 2mm wide and spaced 0.7mm apart were designed with 51.1%, 68.5% and 80.9% porosity. SLS is a thermally based, layered manufacturing process where processing parameters such as part bed temperature, laser power, laser scan speed and laser scan spacing determine the part quality. With sub-optimal processing parameters parts can have a variety of defects: dimensional inaccuracies due to excess bonding of powder to the part's surface, low part

NIH-PA Author Manuscript

NIH-PA Author Manuscript

NIH-PA Author Manuscript

density due to incomplete melting of powder inside of the designed solid regions, and incomplete bonding between layers followed by delamination. Optimal SLS parameters were chosen for each PCL:HA composite material system (Table 1) using the same methodology that has been described previously [12].

Mechanical Properties

Mechanical testing was conducted in accordance with ASTM standard D695 Type 2a. A MTS Alliance RT30 test frame (MTS Systems Corp., Eden Prairie, MN) was used for compression testing. Specimens were compressed to 50% strain between two steel plates at a rate of 1 mm/min after an initial preload of 6.7 N (1.5 lb) was applied. The mechanical properties reported for the orthogonally porous scaffold specimens correspond to effective values of stress and strain.

Finite Element Analysis

In order to predict the mechanical properties of the composite scaffolds for any loading of HA, a three stage process based on first principles modeling was used (Figure 2). A random sphere packing model was employed to model the distribution of HA particulates in sintered PCL matrix. The location data from the packing model was then exported to a micromechanical model to predict the mechanical properties of the bulk material. The predictions of the bulk properties were then used to determine the mechanical properties of the full-sized scaffolds.

A random sphere packing model similar to that of Jodrey et al. [32] was implemented in MATLAB. Briefly, fifty HA particles, each considered as a sphere with radius 25 μm, were randomly placed in a bounding box with a volume equal to the combined volume of all the HA particles (3.2725e6 μm^3). The particles were initially allowed to overlap and then they were iteratively moved apart by an increment of λ until they no longer overlapped. The increment λ was varied from 1 to 100 μm on a log scale with 100 samples. The distribution of packing fractions over the range of input values for λ are shown in Figure 3. Packing fractions as high as 0.55 were obtained using this method.

The particle locations from the random sphere packing model were then imported into COMSOL as input for the micromechanical model. For each simulation of this model a representation of the HA particles in a PCL matrix was created and meshed. HA particles occurring partially outside the bounding box were cropped to only include the volume remaining inside. Meshes varied in size from 16113 to 32507 elements based on the loading percent of HA and other factors arising from the random nature of the simulations. Boundary conditions were specified at two opposite faces with one being held fixed and the other being displaced to an axial strain (compression) of 0.01. The simulation was then solved using a linear stationary solver and the reaction force at the fixed end was evaluated to solve for the elastic modulus using Hooke's Law. The 5 randomly generated geometries were strained in the x, y and z directions one at a time and then averaged to find the average elastic modulus for each material system.

Lastly, stiffness constants for the porous scaffolds were calculated in a macroscale finite element model by using COMSOL Multiphysics (COMSOL Group, Stockholm, Sweden) and compared to the results from the mechanical testing of scaffolds with designed porosity. The testing geometries were imported directly into the Structural Mechanics Module in COMSOL. The models were meshed using 6814, 16510 and 46568 tetrahedral elements for D695-1D, D695-2D and D695-3D respectively. The elastic moduli determined from the micromechanical modeling of the PCL:HA composite material systems were used as the bulk elastic modulus for the scaffolds. The effective elastic moduli of the scaffolds were

NIH-PA Author Manuscript

NIH-PA Author Manuscript

NIH-PA Author Manuscript

computed similarly to the micromechanical simulations with the exception that they were only strained along their long axis.

Material properties were assumed homogenous and isotropic based on optical microscopy [12], mechanical testing (Table 2), and previous FEA on SLS-processed PCL [11, 33]. The elastic modulus of PCL (299.3 MPa) was determined from compression testing of solid gage pure PCL specimens. The elastic modulus of HA (3.69 GPa) was determined using a Hysitron TriboIndenter® (Eden Prairie, MN) to perform single nanoindentations. The Poisson's ratio was assumed to be 0.3.

RESULTS AND DISCUSSION

Scaffold Fabrication

Processing parameters (Table 1) were chosen to reach the highest level of densification and dimensional accuracy. The HA acted as an anti-caking agent at temperatures close to the melting temperature for the neat polymer and allowed for a higher part bed temperature to be used for the composite than the neat polymer. Loading with a high melting point filler, such as HA, causes an increase in the viscosity of the melt pool during SLS processing and can sometimes cause a decrease in part density; however in this study, near-full density was achieved (>99%) in the designed solid regions of the scaffolds as determined by planar-area void fraction analysis of cross-sectional optical micrographs. Further inspection of scaffold cross-sections using SEM confirmed the high part density (Figure 4). No delamination was observed even at 30% HA loading indicating good bonding between the polymer matrix and HA particles.

Mechanical Properties

The compressive mechanical property measurements of SLS-processed solid and designed porous PCL:HA specimens are listed in Table 2. An overall improvement in compressive modulus (E) was observed with the inclusion of HA in almost all cases. A significant difference ($n=5$, $p<0.05$) was not observed in the compressive modulus of solid gage samples when comparing pure PCL to the 10% loaded PCL:HA composite samples. In the case of the 1D, 2D and 3D scaffold specimens, a significant difference ($n=5$, $p<0.05$) was observed in every case when comparing the effective compressive modulus of the corresponding pure PCL (100:0) scaffolds to the 90:10, 80:20 and 70:30 PCL:HA composite scaffolds. In summary, a significant increase in compressive modulus was measured when increasing the HA loading of the composite by as little as 10% in 11 out of the 12 cases.

Solid gage samples showed an increase from 299.3 to 498.3 MPa when increasing the loading of HA from 0 to 30% and in the scaffold with the highest porosity (80.9%), the compressive modulus increased more than 100% (14.9 to 36.2 MPa). The improvement in compressive moduli for the scaffolds can be attributed to particulate reinforcement by the hard-phase HA filler. The ultimate compressive strength (σ_{uc}) and strain at yield (ε_y) of the solid and scaffold specimens did not improve with increased loading of HA.

Finite Element Analysis

Bulk compressive Young's moduli were computed for HA loading at 10, 20 and 30% vol. using a micromechanical model and found to be in good agreement with measurements from mechanical testing of solid gage specimens with an average error of 12.17%. Compressive effective moduli for the porous scaffold geometries were predicted by FEA and also closely agreed with the results from mechanical testing with an average of 25.65% error. FEA predictions of compressive effective elastic moduli for both solid and porous specimens are shown in Figure 5.

NIH-PA Author Manuscript

NIH-PA Author Manuscript

NIH-PA Author Manuscript

Plots of von Mises stress distributions for the porous scaffolds are shown in Figure 6. Stresses were evenly distributed in the 1D scaffold case. There were stress concentrations at the corners of the columns of the 2D and 3D scaffolds. In the areas of the high stress concentration, the von Mises stress did not exceed the yield stress for the bulk material.

The average error of the FEA of PCL:HA composites reported here is better than what we have shown recently for pure PCL (error of 30%) [13]. It is also lower than what has been reported in the literature by Williams et al. [11] (100% error) and Cahill et al. [19] (67% error).

CONCLUSIONS

In this study, we further establish the ability of SLS to manufacture PCL:HA composite scaffolds with near-full density in designed solid regions for bone tissue engineering. The mechanical properties of the PCL:HA composites showed improvement over that of pure PCL. We also demonstrate that the mechanical properties of these scaffolds can be predicted before manufacturing with high accuracy. A direct extension of being able to predict the mechanical properties of composite materials at any filler loading in combination with a direct fabrication method with the capability to produce complex anatomic parts is the ability to custom design both the material properties and the anatomic shape of tissue engineered constructs for both patient and site-specific recovery strategies.

Acknowledgments

This work was funded by the National Institute of Dental and Craniofacial Research (NIDCR) of the National Institutes of Health (NIH) under grant 5R21DE014736-02.

REFERENCES

1. Deckard, CR. Mechanical Engineering. University of Texas at Austin; Austin: 1988. Selective Laser Sintering.
2. Cesarano J III, et al. Customization of Load-Bearing Hydroxyapatite Lattice Scaffolds. International Journal of Applied Ceramic Technology. 2005; 2(3):212–220.
3. Dyson JA, et al. Development of Custom-Built Bone Scaffolds Using Mesenchymal Stem Cells and Apatite-Wollastonite Glass-Ceramics. Tissue Engineering. 2007; 13(12):2891–2901. [PubMed: 17764401]
4. Hutmacher DW, Sittinger M, Risbud MV. Scaffold-based tissue engineering: rationale for computer-aided design and solid free-form fabrication systems. Trends in Biotechnology. 2004; 22(7):354–362. [PubMed: 15245908]
5. Jiankang H, et al. Custom fabrication of composite tibial hemi-knee joint combining CAD/CAE/CAM techniques. Proceedings of the Institution of Mechanical Engineers, Part H: Journal of Engineering in Medicine. 2006; 220(8):823–830.
6. Moroni, L., et al. Finite Element Analysis of Meniscal Anatomical 3D Scaffolds: Implications for Tissue Engineering. 2007.
7. Popov VK, et al. Laser technologies for fabricating individual implants and matrices for tissue engineering. J. Opt. Technol. 2007; 74(9):636–640.
8. Saijo H, et al. Maxillofacial reconstruction using custom-made artificial bones fabricated by inkjet printing technology. Journal of Artificial Organs. 2009; 12(3):200–205. [PubMed: 19894095]
9. Wu G, et al. Selective laser sintering technology for customized fabrication of facial prostheses. The Journal of Prosthetic Dentistry. 2008; 100(1):56–60. [PubMed: 18589076]
10. Melchels, FPW., et al. Progress in Polymer Science. Additive manufacturing of tissues and organs. In Press, Corrected Proof
11. Williams JM, et al. Bone tissue engineering using polycaprolactone scaffolds fabricated via selective laser sintering. Biomaterials. 2005; 26(23):4817–4827. [PubMed: 15763261]

NIH-PA Author Manuscript

NIH-PA Author Manuscript

NIH-PA Author Manuscript

12. Partee B, Hollister SJ, Das S. Selective laser sintering process optimization for layered manufacturing of CAPA® 6501 polycaprolactone bone tissue engineering scaffolds. Journal of Manufacturing Science and Engineering, Transactions of the ASME. 2006; 128(2):531–540.
13. Eshraghi S, Das S. Mechanical and microstructural properties of polycaprolactone scaffolds with one-dimensional, two-dimensional, and three-dimensional orthogonally oriented porous architectures produced by selective laser sintering. Acta Biomaterialia. 2010; 6(7):2467–2476. [PubMed: 20144914]
14. Hench LL, Polak JM. Third-Generation Biomedical Materials. Science. 2002; 295(5557):1014–1017. [PubMed: 11834817]
15. Shor L, et al. Fabrication of three-dimensional polycaprolactone/hydroxyapatite tissue scaffolds and osteoblast-scaffold interactions in vitro. Biomaterials. 2007; 28(35):5291–5297. [PubMed: 17884162]
16. Laurencin CT, et al. Tissue engineered bone-regeneration using degradable polymers: The formation of mineralized matrices. Bone. 1996; 19(1, Supplement 1):S93–S99.
17. Ma PX, et al. Engineering new bone tissue in vitro on highly porous poly(α-hydroxyl acids)/hydroxyapatite composite scaffolds. Journal of Biomedical Materials Research. 2001; 54(2):284–293. [PubMed: 11093189]
18. Guarino V, et al. The role of hydroxyapatite as solid signal on performance of PCL porous scaffolds for bone tissue regeneration. Journal of Biomedical Materials Research Part B: Applied Biomaterials. 2008; 86B(2):548–557.
19. Chim H, et al. A comparative analysis of scaffold material modifications for load-bearing applications in bone tissue engineering. International Journal Of Oral And Maxillofacial Surgery. 2006; 35(10):928–934. [PubMed: 16762529]
20. Eosoly S, et al. Selective laser sintering of hydroxyapatite/poly-ε-caprolactone scaffolds. Acta Biomaterialia. 2010; 6(7):2511–2517. [PubMed: 19616649]
21. Eosoly S, Lohfeld S, Brabazon D. Effect of Hydroxyapatite on Biodegradable Scaffolds Fabricated by SLS. Key Eng Mater. 2009; 396:398.
22. Azevedo MC, et al. Development and properties of polycaprolactone/hydroxyapatite composite biomaterials. Journal of Materials Science: Materials in Medicine. 2003; 14(2):103–107. [PubMed: 15348480]
23. Wiria FE, et al. Poly-ε-caprolactone/hydroxyapatite for tissue engineering scaffold fabrication via selective laser sintering. Acta Biomaterialia. 2007; 3(1):1–12. [PubMed: 17055789]
24. Domingos M, et al. Effect of process parameters on the morphological and mechanical properties of 3D Bioextruded poly (ε-caprolactone) scaffolds. Rapid Prototyping Journal. 2011; 18(1):56–67.
25. Shor L, et al. Solid Freeform Fabrication of Polycaprolactone/Hydroxyapatite Tissue Scaffolds. Journal of Manufacturing Science & Engineering. 2008; 130:1–6.
26. Lam CXF, Teoh SH, Hutmacher DW. Comparison of the degradation of polycaprolactone and polycaprolactone-(β-tricalcium phosphate) scaffolds in alkaline medium. Polymer International. 2007; 56(6):718–728.
27. Perstorp. Biodegradable CAPA Thermoplastics. 2003.
28. Chung H, Das S. Processing and properties of glass bead particulate-filled functionally graded Nylon-11 composites produced by selective laser sintering. Materials Science and Engineering: A. 2006; 437(2):226–234.
29. Chung H, Das S. Functionally graded Nylon-11/silica nanocomposites produced by selective laser sintering. Materials Science and Engineering: A. 2008; 487(1–2):251–257.
30. Athreya SR, Kalaitzidou K, Das S. Processing and characterization of a carbon black-filled electrically conductive Nylon-12 nanocomposite produced by selective laser sintering. Materials Science and Engineering: A. 2010; 527(10–11):2637–2642.
31. Athreya SR, Kalaitzidou K, Das S. Mechanical and microstructural properties of Nylon-12/carbon black composites: Selective laser sintering versus melt compounding and injection molding. Composites Science and Technology. 2010
32. Jodrey W, Tory E. Computer simulation of close random packing of equal spheres. Physical review A. 1985; 32(4):2347. [PubMed: 9896349]

33. Cahill S, Lohfeld S, McHugh P. Finite element predictions compared to experimental results for the effective modulus of bone tissue engineering scaffolds fabricated by selective laser sintering. Journal of Materials Science: Materials in Medicine. 2009; 20(6):1255–1262. [PubMed: 19199109]

NIH-PA Author Manuscript

NIH-PA Author Manuscript

NIH-PA Author Manuscript

NIH-PA Author Manuscript

NIH-PA Author Manuscript

NIH-PA Author Manuscript

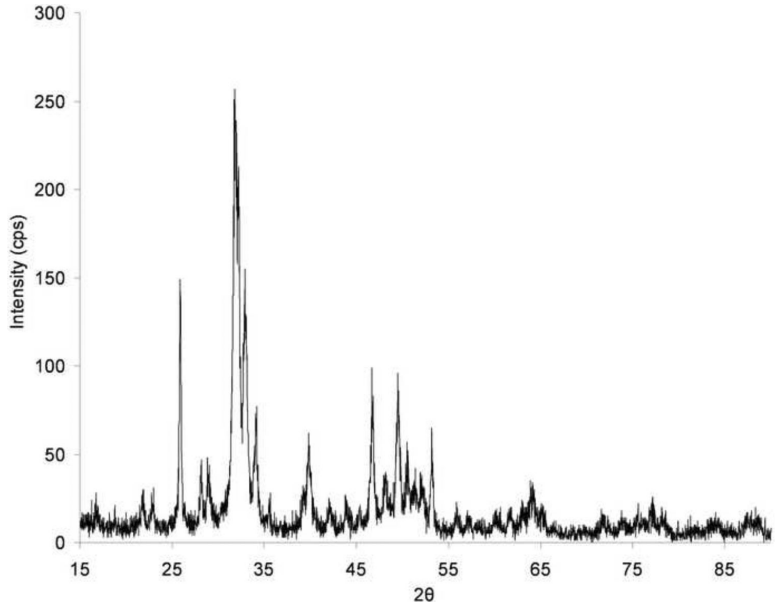

Figure 1.
X-ray diffraction pattern for hydroxyapatite powder

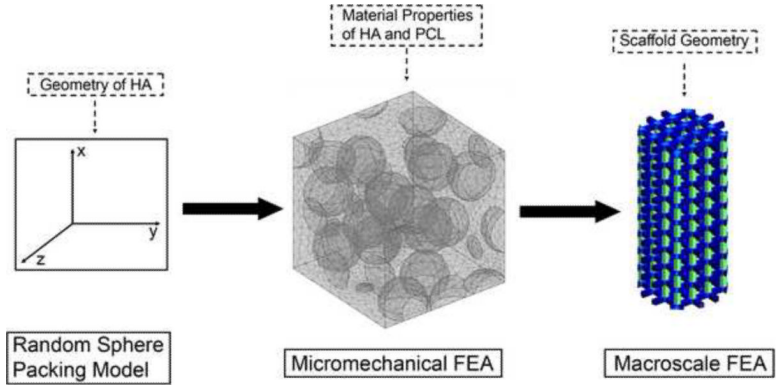

Figure 2.
Diagram of the three-stage modeling process to predict the mechanical properties of PCL:HA scaffolds at any filler loading

NIH-PA Author Manuscript
NIH-PA Author Manuscript
NIH-PA Author Manuscript

NIH-PA Author Manuscript

NIH-PA Author Manuscript

NIH-PA Author Manuscript

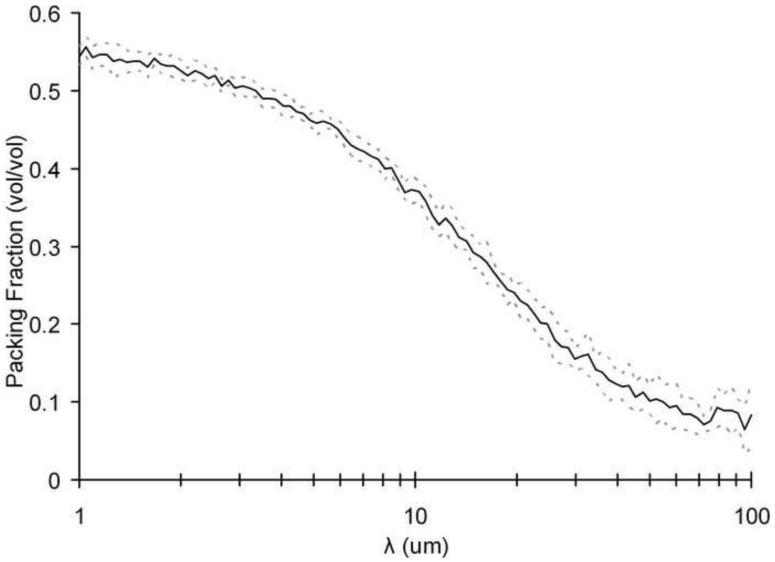

Figure 3.
Distribution of packing fractions from random sphere packing model over a given range of input values for step size λ (n=10; dashed lines indicate standard deviation)

NIH-PA Author Manuscript

NIH-PA Author Manuscript

NIH-PA Author Manuscript

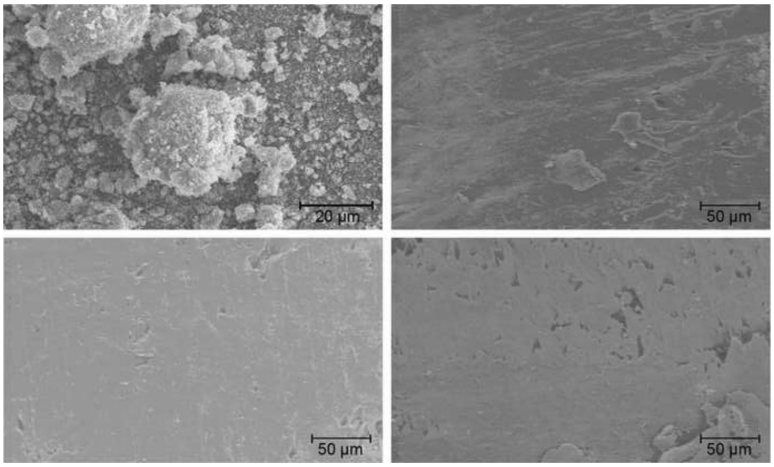

Figure 4.
Scanning electron microscope images of pure HA powder and SLS-processed PCL:HA composites; HA powder (top left), SLS-processed 90:10 (top right), SLS-processed 80:20 (bottom left). SLS-processed 70:30 (bottom right)

NIH-PA Author Manuscript

NIH-PA Author Manuscript

NIH-PA Author Manuscript

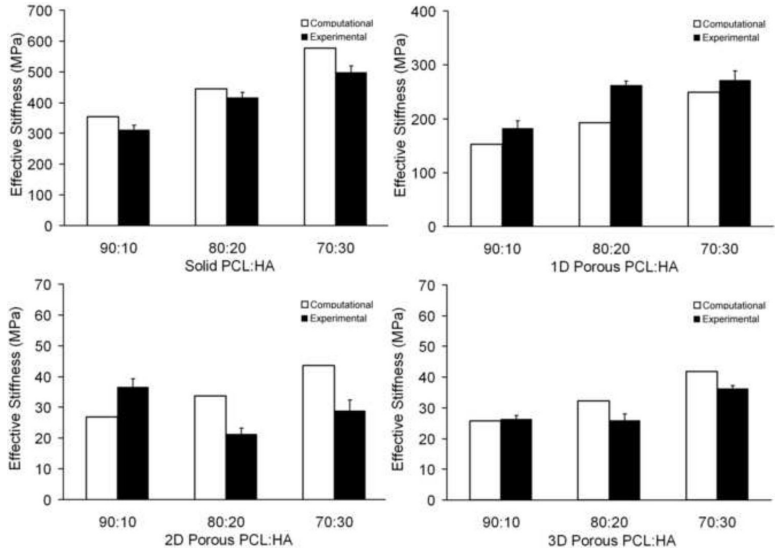

Figure 5.

Experimental and computational compressive effective elastic moduli for 90:10, 80:20 and 70:30 PCL:HA composites; (top-left) solid, (top-right) 1D porous, (bottom-left) 2D porous, (bottom-right) 3D porous (error bars denote standard deviation; n=5)

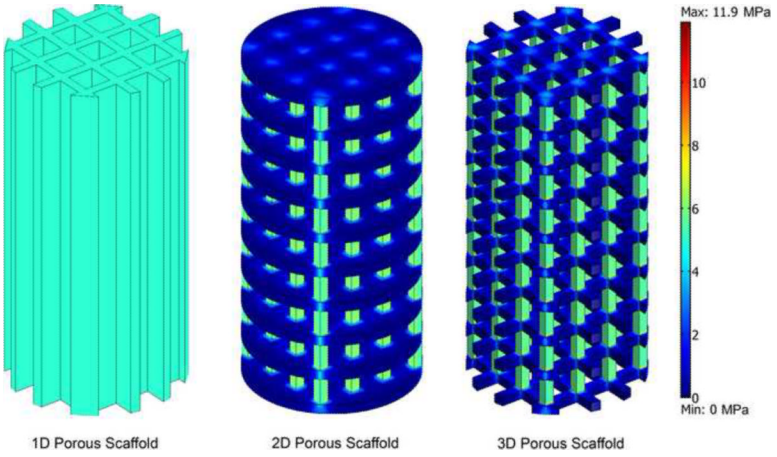

Figure 6.
von Mises stress plots for porous compressive scaffold geometries; (left) 1D porous, (center) 2D porous and (right) 3D porous scaffolds for PCL:HA 70:30

NIH-PA Author Manuscript
NIH-PA Author Manuscript
NIH-PA Author Manuscript

NIH-PA Author Manuscript

NIH-PA Author Manuscript

NIH-PA Author Manuscript

Table 1

Optimal selective laser sintering processing parameters for PCL:HA (ratios indicate volume) and part density

Parameter	Setting		
	90:10	**80:20**	**70:30**
Laser power	1W	1W	1.2W
Scan speed	914 mm/s	914 mm/s	914 mm/s
Scan spacing	152.4 μm	152.4 μm	152.4 μm
Part bed temperature	50 °C	50 °C	50 °C
Part Density	99.8%	99.5%	99.6%

NIH-PA Author Manuscript NIH-PA Author Manuscript NIH-PA Author Manuscript

Table 2

Mechanical property assessment of bulk and porous SLS-processed PCL:HA (ratios indicate volume)

PCL:HA	Property	Unit	Solid gage Section	Porous gage section		
				1D	2D	3D
100:0	Elastic Modulus, E	MPa	299.3 ± 4.6	133.4 ± 1.3	12.1 ± 0.2	14.9 ± 0.3
	Strain at yield, ε_Y	–	0.052 ± 0.001	0.037 ± 0.000	0.038 ± 0.000	0.027 ± 0.002
	Ultimate Compressive Strength, σ_{UC}	MPa	34.5 ± 0.1	10.0 ± 0.3	0.7 ± 0.2	0.6 ± 0.0
90:10	Elastic Modulus, E	MPa	311.2 ± 15.1	182.6 ± 13.1	36.6 ± 2.7	26.4 ± 1.1
	Strain at yield, ε_Y	–	0.054 ± 0.006	0.047 ± 0.007	0.034 ± 0.005	0.027 ± 0.002
	Ultimate Compressive Strength, σ_{UC}	MPa	33.7 ± 1.0	10.8 ± 0.3	2.4 ± 0.8	0.8 ± 0.05
80:20	Elastic Modulus, E	MPa	415.5 ± 17.6	261.9 ± 8.3	21.2 ± 2.0	25.9 ± 2.1
	Strain at yield, ε_Y	–	0.037 ± 0.002	0.045 ± 0.003	0.04 ± 0.02	0.034 ± 0.008
	Ultimate Compressive Strength, σ_{UC}	MPa	32.0 ± 1.0	14.5 ± 0.8	1.9 ± 0.3	1.0 ± 0.1
70:30	Elastic Modulus, E	MPa	498.3 ± 21.8	271.9 ± 17.3	28.8 ± 3.5	36.2 ± 1.0
	Strain at yield, ε_Y	–	0.050 ± 0.006	0.033 ± 0.003	0.037 ± 0.02	0.026 ± 0.005
	Ultimate Compressive Strength, σ_{UC}	MPa	24.6 ± 0.8	10.6 ± 0.7	1.5 ± 0.1	0.9 ± 0.3

Acta Biomater. Author manuscript; available in PMC 2013 August 01.